

Flight-Test Evaluation of Integer Ambiguity Resolution Enabled PPP

Ma, Hongyang; Verhagen, Sandra; Psychas, Dimitrios; Monico, João Francisco Galera; Marques, Haroldo Antonio

DOI

[10.1061/\(ASCE\)SU.1943-5428.0000367](https://doi.org/10.1061/(ASCE)SU.1943-5428.0000367)

Publication date

2021

Document Version

Accepted author manuscript

Published in

Journal of Surveying Engineering

Citation (APA)

Ma, H., Verhagen, S., Psychas, D., Monico, J. F. G., & Marques, H. A. (2021). Flight-Test Evaluation of Integer Ambiguity Resolution Enabled PPP. *Journal of Surveying Engineering*, 147(3), Article 04021013. [https://doi.org/10.1061/\(ASCE\)SU.1943-5428.0000367](https://doi.org/10.1061/(ASCE)SU.1943-5428.0000367)

Important note

To cite this publication, please use the final published version (if applicable).
Please check the document version above.

Copyright

Other than for strictly personal use, it is not permitted to download, forward or distribute the text or part of it, without the consent of the author(s) and/or copyright holder(s), unless the work is under an open content license such as Creative Commons.

Takedown policy

Please contact us and provide details if you believe this document breaches copyrights.
We will remove access to the work immediately and investigate your claim.

Flight-test evaluation of integer ambiguity resolution enabled PPP

Mr. Hongyang Ma (mahy@whu.edu.cn),
Department of Geoscience and Remote Sensing, Delft University of Technology, Delft, The Netherlands.

Dr. Sandra Verhagen (sandra.verhagen@tudelft.nl),
Department of Geoscience and Remote Sensing, Delft University of Technology, Delft, The Netherlands.

Mr. Dimitrios Psychas (d.psychas@fugro.com)
Fugro Innovation & Technology B.V., Leidschendam, The Netherlands.

Prof. Dr. João Francisco Galera Monico (galera.monico@unesp.br)
Departamento de Engenharia Cartográfica, Universidade Estadual Paulista Júlio de Mesquita Filho (UNESP), Presidente
Prudente - SP, Brasil.

Dr. Haroldo Antonio Marques (haroldoh2o@gmail.com)
Seção de Engenharia Cartográfica, Instituto Militar de Engenharia (IME), Rio de Janeiro - RJ, Brasil.

* Corresponding author: H. Ma (mahy@whu.edu.cn)

ABSTRACT

The technology of integer ambiguity resolution enabled precise point positioning (also referred to as PPP-AR) has been proven capable of providing comparable accuracy, efficiency and productivity to long-baseline Real-Time Kinematic positioning (RTK) during the last decade. Commercial PPP-AR services have been provided by different institutions and companies and have been widely used in geodetic missions. However, the usage and research of the PPP-AR mostly concentrated on nonaviation applications, e.g., vehicle navigation, surveying and mapping and monitoring crustal motions. Few of them focused on fixing the ambiguities during an aircraft flight. In this contribution, we implemented the PPP-AR technique for the first time in an airplane flight test to investigate how much the fixed ambiguities could contribute to airplane positioning solutions in the challenging circumstances, including high velocity and severe maneuver. We first looked into the influences of the tropospheric delay on the positioning and ambiguity solutions since the height of the airplane may dramatically change within a narrow time span, and thus a proper constraint of this parameter was crucial for the computation of the tropospheric effects. Then how to fix the ambiguities successfully and reliably in the

29 challenging circumstances was discussed. Finally, the airplane data was processed in 15 s and 1 s
30 interval with ambiguity float and fixed solution under different configurations to illustrate in which
31 condition and to what extent the fixed ambiguities can improve the airplane positioning accuracy.

32 Keywords: GNSS; PPP; PPP-AR; Integer ambiguity resolution; Airplane navigation

33 INTRODUCTION

34 Global Navigation Satellite System (GNSS) has provided an unprecedented high accuracy,
35 flexibility and tremendous contribution to navigation, timing and scientific issues related to precise
36 positioning on Earth's surface (Teunissen and Kleusberg 2012). As one of its important applications,
37 precise point positioning (PPP) uses undifferenced pseudo-range and carrier phase observations along
38 with precise satellite orbit and clock products for standalone kinematic and static positioning (Zumberge
39 et al. 1997; Kouba and Héroux 2001). Nowadays PPP has become an essential tool for providing
40 position information to personal navigation (Wu et al. 2019; Psychas et al. 2019), vehicle and machinery
41 control (Prabha et al. 2014), location-based monitoring (Richter et al. 2016), maritime operations (Ma et
42 al. 2017) and cooperative mobility (Severi et al. 2018).

43 Among others, aircraft navigation by means of PPP has been widely studied, and the number of
44 aircraft including airplanes and unmanned aerial vehicles (UAV) equipped with GNSS receiver chipset
45 is increasing. Monico et al. (2019) implemented real-time PPP methodology in two airplane flight tests
46 and found that the accuracy of 30 cm for the horizontal and 50 cm for the vertical component can be
47 achieved in the use of GPS real-time orbit and clock products as compared to the relative positioning
48 solutions. Teunissen et al. (2011) proposed a new algorithm for GNSS attitude determination and
49 analyzed its performance in different platforms, including ground, maritime and airplane. The flight test
50 results showed that the aircraft attitudes obtained from PPP compared very well with the precise relative
51 attitude determination results, and the differences mostly contained within 0.2° .

52 Dorn et al. (2015) applied the PPP concept to the remotely piloted aircraft system (PARS) to obtain
53 the position and velocity. However, their results were based on a driving-simulating-flying test which
54 was much easier to verify the positioning solutions. And PPP was proved to achieve decimeter-level
55 accuracy in the experiment. Roberts et al. (2005) investigated the synergies that exist between GNSS
56 and vision for fixed-wing UAV navigation and control applications. The simulation test results
57 presented that the root mean square (RMS) errors of roll, pitch and yaw angle are approximate 0.5° .
58 Imparato (2016) monitored the integrity of the navigation systems on an aircraft by exploiting the
59 redundancy of the GNSS signals as collected at the receiver.

60 Although GNSS has been widely implemented in aircraft navigation, one of the bottlenecks is that
61 the carrier-phase cannot contribute to the positioning solutions in the sense of fast and high-precision
62 PPP parameter estimation because the ambiguities are not able to preserve their integer nature due to the
63 presence of the satellite and receiver phase biases (Teunissen 1998a); and thus the standard PPP cannot
64 perform integer ambiguity resolution. During the last decade, several methods which enable PPP to
65 achieve integer ambiguity resolutions have been proposed and formulated (Ge et al. 2008; Teunissen et
66 al. 2010; Geng et al. 2011; Li et al. 2013), and this integer ambiguity resolution enabled PPP is referred
67 to as PPP-AR. These PPP-AR methods differing in the used model and applied corrections, as well as
68 their connections, were reviewed by Teunissen and Khodabandeh (2015).

69 Generally, two types of combination methodology for pseudo-range and carrier phase are mainly
70 used in PPP-AR: ionosphere-free combination and uncombined observable (Odijk 2003; Odijk et al.
71 2016). Each combination has its own advantages in data processing and will give exactly the same
72 solution when rigorously solved. In this study we prefer using the uncombined observable because it is
73 flexible for further model strengthening, i.e., strengthened by the external ionospheric pseudo observable.
74 Besides, the advantages of the uncombined observable also include the simplest observation variance-

75 covariance matrix, and all parameters are available for scientific research. Teunissen et al. (2010)
76 proposed an uncombined PPP-AR model by means of reparametrizing the undifferenced GNSS
77 observation equations so as to eliminate the rank defects. And the results indicated that PPP-AR works
78 very much like network RTK if precise ionospheric corrections are made available to the user.

79 Since then, Zhang et al. (2011) extended the usage of the undifferenced and uncombined PPP-AR to
80 a sparse ground network since the ionospheric effects were considered in the functional model. Odijk et
81 al. (2014) focused on the single-frequency PPP-AR application and proved that single-frequency PPP
82 integer ambiguity resolution is feasible in less than 10 min when applying the ionosphere corrections in
83 a small network. Nadarajah et al. (2018) provided numerical insights into the role taken by the multi-
84 GNSS integration in delivering fast and high-precision positioning solutions using uncombined PPP-AR
85 model.

86 Except for the scientific research, companies also provide commercial products such as satellite
87 phase biases and ionospheric corrections along with satellite orbit and clock products to users to help
88 them fix the integer ambiguities. For instance, Trimble RTX service offers flexible subscription options
89 in order to meet user's requirements from meter to centimeter level (Chen et al. 2011; Alkan 2019).
90 Fugro G2+ provides clients with the additional hardware biases that are computed using global reference
91 stations to enhance positioning services with integer ambiguity resolved PPP for two GNSSs (GPS and
92 GLONASS) and G4 provides the ambiguity float solutions for four GNSSs (GPS, GLONASS, Galileo
93 and BDS) (Liu et al. 2015; Tegedor et al. 2016).

94 Although PPP-AR has been widely implemented in scientific research and industrial applications,
95 few publications focus on fixing the ambiguities on aircraft due to the challenging circumstances,
96 including high velocity and severe maneuver. In this contribution, we implement the PPP-AR technique
97 for the first time in an airplane flight test to investigate to what extent the fixed ambiguities could

98 contribute to airplane positioning solutions. Besides, several key issues related to the positioning and
99 ambiguity solutions are also discussed. We first investigate the influence of the tropospheric delays on
100 PPP-AR estimations because a tight constraint is always given to this parameter for nonaviation
101 applications based on the stable troposphere behavior on the ground. However, this is not the case for
102 the aircrafts whose altitude may dramatically change within a narrow time span. Therefore, a proper
103 constraint needs to be considered for the tropospheric delay.

104 Then different values of the success rate criterion of integer ambiguity resolution (Teunissen 2000)
105 are assessed; as it is well known that both strength of underlying model and accuracy of float
106 ambiguities are crucial factors for successful and reliable ambiguity fixing in real applications (Li et al.
107 2014), and the success rate represents the model strength to some extent. Therefore, we believe that a
108 higher success rate criterion would be helpful to obtain the correct fixed ambiguities because wrongly
109 resolved integer ambiguities may result in unacceptably large position errors (Verhagen et al. 2013).
110 However, the higher success rate also means longer waiting time to get the first integer ambiguity
111 solution.

112 Finally, the airplane data is processed in 15 s and 1 s interval with ambiguity float and fixed
113 solutions under different configurations to illustrate in which condition and to what extent the fixed
114 ambiguities can improve the airplane positioning accuracy. The reason for the 15 s interval data
115 processing is that as mentioned before, the satellite phase bias corrections are needed for integer
116 ambiguity resolution, and we generate these corrections as well as the satellite clock corrections through
117 a GNSS network in the interval of 15 s. This also means that 1 s corrections need to be interpolated to
118 meet the requirement of the data processing. Thus, the performance of the interpolated corrections is
119 another focus of this contribution.

120 This article is organized as follows. An undifferenced and uncombined PPP-AR model at both
 121 network and user side is provided in the next section, as well as a brief description of the theory of
 122 integer ambiguity resolution. In the third section, a GNSS network with 20 reference stations is selected,
 123 and the airplane data is processed in ambiguity float and fixed solutions, respectively. The key issues
 124 mentioned above are also discussed in this section. The final section gives conclusions and remarks of
 125 this research.

126 PPP-AR THEORY AND INTEGER AMBIGUITY RESOLUTION

127 PPP-AR needs a GNSS network to process the data of a group of receivers to obtain various
 128 corrections such as satellite phase biases and clock offsets. The linearized undifferenced uncombined
 129 GNSS observation equations read as (Teunissen et al. 2010):

$$\begin{aligned}
 E\{\Delta\phi_{r,j}^s\} &= g_r^{sT} \Delta x_r + m_r^s \tau_r - \mu_j t_r^s + dt_r - dt^s + \delta_{r,j} - \delta_{j,j}^s + \lambda_j a_{r,j}^s \\
 E\{\Delta p_{r,j}^s\} &= g_r^{sT} \Delta x_r + m_r^s \tau_r + \mu_j t_r^s + dt_r - dt^s + d_{r,j} - d_{j,j}^s
 \end{aligned}
 \tag{1}$$

130 where $E\{\cdot\}$ is the expectation operator; $\Delta\phi_{r,j}^s$ and $\Delta p_{r,j}^s$ are the so-called observed-minus-computed
 131 phase and code observations on frequency j from satellite s to receiver r , in meters; g_r^s the line-of-sight
 132 unit vector from the satellite to the receiver; Δx the increment of the receiver position; τ_r the zenith
 133 tropospheric delay and m_r^s its corresponding mapping function which introduces an elevation-dependent
 134 scaling factor for each satellite; t_r^s the slant ionospheric delay on the first frequency and having μ_j as the
 135 coefficient; dt_r and dt^s are the receiver and satellite clock offsets, respectively; note that they are
 136 common to both phase and code observation. $\delta_{r,j}$ and $\delta_{j,j}^s$ are the receiver and satellite phase biases, in
 137 meters; $d_{r,j}$ and $d_{j,j}^s$ are the receiver and satellite code biases; λ_j the wavelength and $a_{r,j}^s$ the integer
 138 ambiguity, in cycles.

139 However, the system of observation equations based on Eq. 1 is rank-deficient. To make it a full
 140 rank model, the S -system theory is applied to constrain a set of parameters as the S -basis. Examples of

141 the applicability of this theory to PPP-AR can be found in (Odijk et al. 2017; Ma et al. 2020), and the
 142 constraint set we used to eliminate the rank deficiency is given by

$$\left\{ \begin{array}{l} \text{Pivot receiver clock: } dt_p \\ \text{Receiver and satellite code biases: } d_{r,j} \text{ and } d_{j}^s, \quad r = 1, \dots, n, \quad j = 1,2 \\ \text{Pivot receiver phase biases: } \delta_{p,j}, \quad j = 1,2 \\ \text{Pivot receiver ambiguities: } a_{p,j}^s, \quad s = 1, \dots, m, \quad j = 1,2 \\ \text{Pivot satellite ambiguities: } a_{r,j}^p, \quad r = 2, \dots, n, \quad j = 1,2 \end{array} \right. \quad (2)$$

143 It is worth mentioning that the choice of constraints is not unique, and after resolving the rank-
 144 deficient problem, some of the parameters, e.g., satellite clock offsets and phase biases do not represent
 145 their original parameters anymore. Instead, the estimable parameters are established by the combination
 146 of the original parameters and the constraints. Note that both receiver and satellite code biases are
 147 selected as the S -basis, indicating that these parameters will be absent in the rephrased observation
 148 equations. After reparametrizing Eq. 1 by means of the constraints of Eq. 2, the full rank observation
 149 equations can be constructed as:

$$\begin{aligned} E\{\Delta\phi_{r,j}^s\} &= g_r^{sT} \Delta x_r + m_r^s \tau_r - \mu_j \tilde{l}_r^s + d\tilde{t}_r - d\tilde{t}^s + \tilde{\delta}_{r,j} - \tilde{\delta}_{j}^s + \lambda_j \tilde{a}_{r,j}^s \\ E\{\Delta p_{r,j}^s\} &= g_r^{sT} \Delta x_r + m_r^s \tau_r + \mu_j \tilde{l}_r^s + d\tilde{t}_r - d\tilde{t}^s \end{aligned} \quad (3)$$

150 The arguments \tilde{l}_r^s , $d\tilde{t}_r$, $d\tilde{t}^s$, $\tilde{\delta}_{r,j}$, $\tilde{\delta}_{j}^s$ and $\tilde{a}_{r,j}^s$ refer to the same parameter as in Eq. 1, but their
 151 interpretation is different, as they are lumped with the constraints of Eq. 2. For instance, the ambiguity
 152 term $\tilde{a}_{r,j}^s$ is actually a double differenced ambiguity $\tilde{a}_{r,j}^s = a_{r,j}^s - a_{p,j}^s - a_{r,j}^p + a_{p,j}^p$ in which the
 153 superscript and subscript p denote the pivot satellite and receiver, respectively. It is worth noting that the
 154 temporal constraints would change the interpretation of these estimable parameters because additional
 155 rank deficiencies may occur in the absence of dynamic models. One can refer to Odijk et al. (2016) for
 156 more information about the details of solving the rank deficiency problem.

157 The satellite clock offsets and satellite phase delays estimated from Eq. 3 are provided to the user
 158 side, and the satellite orbits are available by an external provider, e.g., International GNSS Service (IGS).
 159 After applying these corrections and the same constraints as the network, the full rank PPP-AR user
 160 model reads:

$$\begin{aligned}
 E\{\Delta\phi_{u,j}^s + d\tilde{t}^s + \tilde{\delta}_{j,j}^s\} \\
 &= g_u^{sT} \Delta x_u + m_u^s \tau_u - \mu_j \tilde{t}_u^s + d\tilde{t}_u + \tilde{\delta}_{u,j} + \lambda_j \tilde{a}_{u,j}^s \quad (4) \\
 E\{\Delta p_{u,j}^s + d\tilde{t}^s\} &= g_u^{sT} \Delta x_u + m_u^s \tau_u + \mu_j \tilde{t}_u^s + d\tilde{t}_u
 \end{aligned}$$

161 One can see that the satellite and receiver phase biases have been separated from the ambiguities so
 162 that they are possible to be fixed into integer values. Since we have obtained the observation equations
 163 in which the ambiguity can preserve the integer nature, in the following, we will fix the float ambiguities
 164 to integer values. To facilitate the interpretation, either network or user positioning equations can be
 165 written in the compact formula

$$E\{y\} = Aa + Bb, \quad D\{y\} = Q_{yy} \quad (5)$$

166 where y represents the vector with phase and code observables; a and A are the ambiguity parameters
 167 and the corresponding design matrix, while b and B are the baseline parameters and design matrix which
 168 include all other parameters except for the ambiguities. $D\{\cdot\}$ denotes the mathematical dispersion
 169 operation, and Q_{yy} refers to the variance matrix of the observation.

170 By applying an estimator, e.g., least-squares or Kalman filter (Verhagen and Teunissen 2017), the
 171 float solutions of ambiguity \hat{a} and position components \hat{b} can be obtained, as well as their individual
 172 variance matrix $Q_{\hat{a}\hat{a}}$ and $Q_{\hat{b}\hat{b}}$, and the covariance matrix $Q_{\hat{a}\hat{b}}$. Then the LAMBDA method (Teunissen
 173 1993, 1995) is used to fix the ambiguities because of its efficiency and optimality. The first step of the
 174 LAMBDA is to transform the highly correlated ambiguities to a new set of decorrelated ambiguities by a
 175 transformation matrix Z^T (Teunissen et al. 1997):

$$\hat{z} = Z^T \hat{a}, \quad Q_{\hat{z}\hat{z}} = Z^T Q_{\hat{a}\hat{a}} Z \quad (6)$$

176 To preserve the integer nature of the ambiguities, the transformation matrix Z^T needs to be integer
 177 and volume preserving. Then the second step is to search the integer values of the float ambiguity in the
 178 space (Teunissen 1996):

$$(\hat{z} - z) Q_{\hat{z}\hat{z}} (\hat{z} - z) \leq \chi^2 \quad (7)$$

179 where $z \in Z^n$, and χ^2 defines a certain searching space instead of the whole integers in Z^n . The optimal
 180 integer estimator is the integer least-squares which has the maximum success rate of fixing ambiguities
 181 (Teunissen 1998b). Therefore, with the integer least-squares solution \check{z} , the ambiguities before
 182 decorrelation can be computed from the back transformation $\check{a} = Z^{-T} \check{z}$. The final step is to provide the
 183 ambiguity fixed baseline solution \check{b} by adjusting the float solution \hat{b}

$$\begin{aligned} \check{b} &= \hat{b} - Q_{\hat{b}\hat{a}} Q_{\hat{a}\hat{a}}^{-1} (\hat{a} - \check{a}) \\ Q_{\check{b}\check{b}} &= Q_{\hat{b}\hat{b}} - Q_{\hat{b}\hat{a}} Q_{\hat{a}\hat{a}}^{-1} Q_{\hat{a}\hat{b}} \end{aligned} \quad (8)$$

184 It is obvious that $Q_{\check{b}\check{b}} \leq Q_{\hat{b}\hat{b}}$, which means the ambiguity fixed baseline estimations are more precise
 185 than those of the ambiguity float. However, it is worth noting that the formula of $Q_{\check{b}\check{b}}$ is not rigorous
 186 since the fixed ambiguity \check{a} is considered as a deterministic parameter here, and hence only acceptable if
 187 the success rate is very close to 1. For more information of taking into account the stochastic property of
 188 \check{a} and how it influences the variance of \check{b} , one can refer to Teunissen (1998c).

189 Both strength of underlying model and accuracy of float ambiguities are two crucial factors for
 190 successful and reliable ambiguity fixing, and the integer ambiguity resolution success rate plays an
 191 important role in measuring the model strength. It has been demonstrated that the bootstrapped
 192 probability of obtaining the correct integer ambiguity vector is the lower bound of the integer least-
 193 squares estimator (Teunissen 2000), which reads as

$$P(\check{\alpha} = a) = \prod_{i=1}^n (2\Phi\left(\frac{1}{2\sigma_{\hat{a}_{i|I}}}\right) - 1) \quad (9)$$

194 where Φ is the standard normal cumulative probability distribution and $\sigma_{i|I}$ is the standard deviation of
 195 ambiguity i , conditioned on all previous ambiguities, indicated by I .

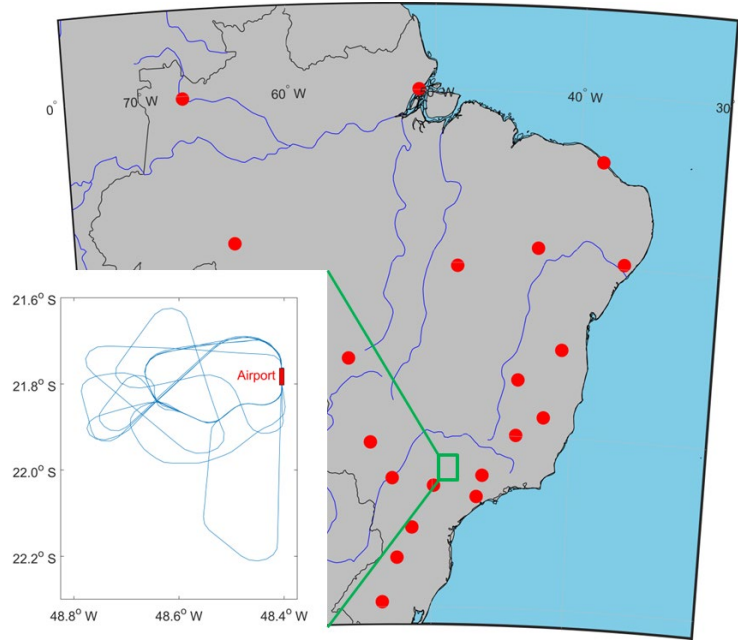
196 Eq. 9 indicates the strength of the float ambiguities, and only in case the success rate is close to one,
 197 the ambiguities can be fixed reliably. Partial integer ambiguity resolution is implemented in the data
 198 processing, which means only a subset of ambiguities is fixed to integer values such that a user-defined
 199 success rate criterion is met, rather than fixing all ambiguities (Verhagen et al. 2011; Hou et al. 2016).
 200 This is because it might require a long time until reliable full ambiguity resolution is achieved, and the
 201 accuracy of the baseline parameters have been improved significantly after some of the ambiguities
 202 getting fixed (Teunissen and Verhagen 2009).

203

204 AIRPLANE DATA TESTS AND ANALYZES

205 As mentioned above, a GNSS network is needed in PPP-AR procedure for providing the satellite
 206 phase bias and clock corrections to users. Fig. 1 shows the network used in this study which contains 20
 207 stations of the Brazilian Active Control Network (Fortes et al. 2009). The flight test was carried out in 1-
 208 Sept-2009 equipped with a NovAtel dual-frequency GPS receiver (Monico et al., 2019). The sample rate
 209 of the flight data is 2 Hz, and the duration is approximate 3 hours. The horizontal trajectory of the
 210 airplane can also be seen in Fig. 1.

211



212
213
214

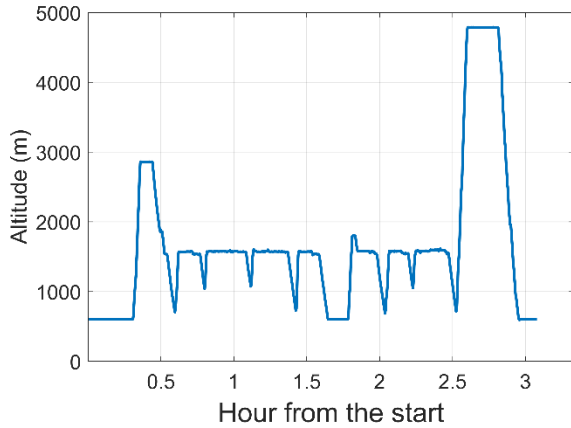
Fig. 1 GNSS network in which the reference stations is represented as the red point and location of the flight test in Sao Paulo State

215
216
217
218
219
220
221
222
223
224
225
226

A reference receiver was set at the airport to collect and store the GNSS data and was employed in the TOPCON-TOOLS commercial software (Gottsmann and del Potro 2008) to generate relative positioning solutions in a forward and backward filtering process with fixed double-differenced ambiguities. Since the baselines between the reference receiver and the airplane are always less than 50 km, these medium-distance relative positioning solutions are believed to be better than or at least comparable to PPP-AR ambiguity fixed positioning solutions, which makes it possible for the relative positioning positions to be regarded as the reference positions of the airplane for verifying the accuracy and the performance of the ambiguity float and fixed solutions of PPP-AR. However, one should keep in mind that the configurations adopted by the TOPCON-TOOLS may influence the performance of the PPP-AR solutions. For example, as the TOPCON-TOOLS implements a tight constraint for the tropospheric delay, the same tight troposphere constraint might be helpful for PPP-AR procedure to fit the TOPCON-TOOLS solutions.

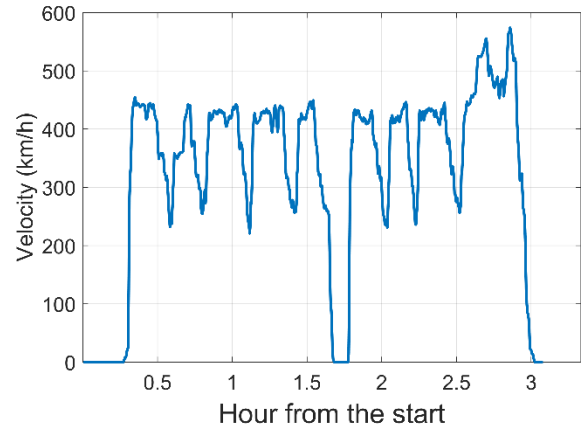
227 Fig. 2 and Fig. 3 present the altitude and velocity of the airplane obtained by the TOPCON-TOOLS
228 during the flight test, respectively. One can see that a series of maneuvers of the airplane, including
229 sudden pushovers, accelerations and s-turns (as can be seen in Fig. 1).

230



231
232

Fig. 2 Altitude of the airplane



233
234

Fig. 3 Velocity of the airplane

235 The data processing strategy options are summarized in Table 1. The flight data are processed in the
236 kinematic mode for which the coordinates are regarded as epoch-independent; meanwhile, the static
237 mode is used for the network by considering the reference stations as stationary sites. GPS constellation
238 with frequencies L1 and L2 is used because the receiver equipped on the airplane is a dual-frequency
239 GPS receiver. The IGS final orbit product is applied in the experiment (Kouba and Héroux 2001)
240 because this study focuses on the performance of the fixed ambiguity positioning solutions; thus, the
241 error sources including the orbit error are to be eliminated as much as possible. A sample rate of 15 s
242 interval is applied first since 15 s interval corrections, including the satellite clock and phase bias
243 corrections for the flight data are generated from the chosen network.

244 Although signals are not likely to be affected by blockages or multipath, satellites at low elevation
245 angles may suffer from unmodelled atmospheric delays. Besides, measurements at low elevation angles
246 would not contribute much to the system since we applied elevation dependent weighting strategy.
247 Those are the reasons why a 10° elevation cutoff angle is chosen, which is the same as we usually use

248 for nonaviation applications. The standard deviations of the phase and code observables are 0.005 m
 249 and 0.5 m, respectively. This is because, typically, the standard deviation of carrier-phase noise is less
 250 than 1 millimeter for a high carrier-to-noise-power-density ratio, and the code measurements are usually
 251 weighted at least 100 times lower than carrier-phase due to their high noises (Teunissen and Kleusberg,
 252 2012).

253 The tropospheric hydrostatic delay is compensated by the Saastamoinen model (Saastamoinen
 254 1972). The forward Kalman filter is implemented in the data processing, therefore, this procedure can be
 255 easily applied in the real-time case as long as the precise real-time orbits are provided. The receiver
 256 clock offsets and slant ionospheric delays are epoch-wise estimation parameters. And the receiver phase
 257 delays and ambiguity parameters are considered as constant according to their behavior in the data
 258 processing. Satellite clock offset and satellite phase delay are absent in the flight data processing as they
 259 are provided as the corrections from the network.

260 Since the purpose of this contribution is to assess the performances of the ambiguity fixed solutions
 261 during a challenging circumstance of an airborne receiver and to investigate how and to what extent the
 262 high velocity and severe maneuver may influence the integer ambiguity resolution, the ratio test is not
 263 implemented into the data processing. Because an improperly selected ratio test procedure may reject
 264 some of the fixed ambiguities, no matter they are wrongly fixed or not. Interested readers are referred to
 265 Verhagen and Teunissen (2004) and Wang and Verhagen (2015) for more information on ratio test.

266
 267 Table 1 Summary of the strategy of data processing for the network and airplane

Parameter	Strategy and value	
	Network	Airplane
Positioning mode	Static	Kinematic
Constellation	GPS	GPS
Frequency	L1 and L2	L1 and L2
Satellite orbits	IGS	IGS
Interval	15 s	15 s and 1 s
Elevation cutoff angle	10°	10°

Weighting strategy	Elevation dependent	Elevation dependent
Standard deviation (STD) of phase/code observable	0.005 m/0.5 m	0.005 m/0.5 m
Zenith hydrostatic delay	Saastamoinen model	Saastamoinen model
Slant ionospheric delay	Epoch by epoch	Epoch by epoch
Kalman filter	Forward	Forward
Receiver clock offset	Epoch by epoch	Epoch by epoch
Satellite clock offset	Epoch by epoch	/
Receiver phase delay	Constant	Constant
Satellite phase delay	Constant	/
Ambiguity	Constant	Constant
Integer ambiguity resolution	Partial	Partial

268

269 Influence of the tropospheric delay on the flight data processing

270 Table 2 shows the RMSs of the ambiguity float positioning solutions with different choices for the
271 tropospheric delay process noises as compared to the reference positions obtained by the relative
272 positioning of TOPCON-TOOLS commercial software. Note that the RMSs are calculated from 0.5 h to
273 the end, during which the positioning solutions should have been converged. One can see that the
274 positioning errors are increasing with the enlarged tropospheric delay process noise, and it becomes
275 especially obvious for the vertical direction. This is because the tropospheric delay and the up
276 component are highly correlated, and therefore the residuals of this type of delay due to the imperfect
277 stochastic model would be mostly lumped into the vertical position.

278 Although the term *positioning errors* is used here and afterwards to assess the performances of PPP-
279 AR with different troposphere process noises, it is actually the *displacements* between the PPP-AR
280 solutions and the reference positions for a rigorous description because the reference might also be
281 affected by GNSS error sources. We only use the *positioning errors* as an idiom for easy understanding.

282 Table 2 RMSs of the ambiguity float positioning solutions in different tropospheric delay process noise

Values (m^2/s)	Ambiguity float solutions (cm)			
	East	North	Horizontal	Up
0.0001	4.51	2.65	5.23	8.79
0.001	4.51	2.65	5.23	8.79
0.01	4.55	2.65	5.26	8.88

0.1

4.55

2.93

5.41

11.28

283

284

285

286

287

288

289

290

291

292

293

294

295

296

297

298

299

300

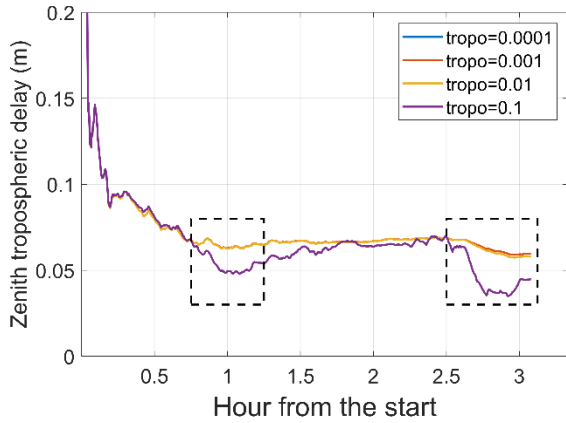
301

302

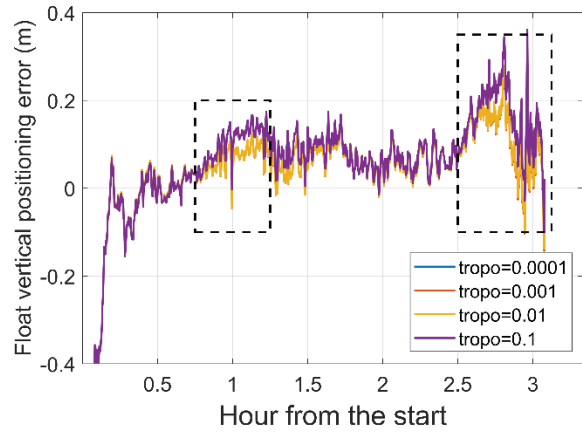
303

Fig. 4 presents the estimates of the tropospheric wet delay in different process noises. It can be seen that the wet delay values are not distinguishable for the tight constraints, i.e., 0.0001, 0.001 and 0.01 m^2/s , and the positioning errors of these three cases are very similar, as shown in Table 2. On the contrary, the loose constraint, 0.1 m^2/s , naturally gives a less stable time series of the wet delay estimation. Big displacements of the troposphere estimates between the loose and tight constraints can be seen in two periods, one is around 1 h, and the other one is from 2.5 to 3 h. Correspondingly, large positioning errors of the up component have appeared in Fig. 5 in the same periods, which means that the loose constraint cannot represent the tropospheric wet delay very well and the impacts of the imperfect modelling are reflected in the vertical positioning errors. Therefore, we use a tight constraint 0.0001 m^2/s in the following data processing.

Table 2 and Fig. 4 indicate that the tropospheric delay parameter needs to be tightly constrained in aviation applications. However, this might be due to the fact that the reference positions from TOPCON-TOOLS are obtained by a tight troposphere constraint, and thus a small troposphere process noise only fits the reference positions well. Even though it is difficult to claim that whether or not a tight troposphere constraint is better than a loose one due to the restriction of lacking airplane's true positions, we can conclude that the horizontal performance of PPP-AR is comparable with the medium-baseline RTK as the maximum distance between the TOPCON-TOOLS reference receiver and the airplane is 50 km. The RMS of the ambiguity float solutions is 5.23 cm with the tight troposphere constraint, and this value is further reduced to 2.52 cm with the ambiguity fixed solutions, as can be seen in Table 3.



304
 305 Fig. 4 Zenith tropospheric wet delay estimations
 306 by different process noises (the unit of the
 307 process noise is m^2/s)



308
 309 Fig. 5 Ambiguity float vertical positioning
 310 errors by different process noises (the unit of the
 311 process noise is m^2/s)

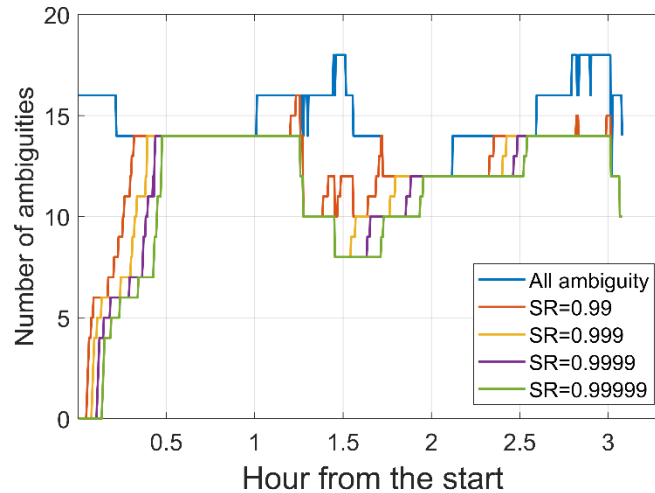
312 Influence of the integer ambiguity resolution success rate on the ambiguity fixed positioning solution

313 The success rate of Eq. 9 with the multiplication of the conditioned standard deviations of
 314 ambiguity is an aspect of the underlying model strength which is an essential factor for successful
 315 integer ambiguity resolution. Since we applied the partial ambiguity resolution, it means that at some
 316 epochs, only a subset of the ambiguity vector can be fixed rather than all ambiguities. In fact, as can be
 317 seen in Fig. 6, the full ambiguity resolution cannot be achieved for most of the processing period
 318 because, on the one hand, a relatively long time is needed since the start of the data processing for the
 319 ambiguities to become precise enough to get fixed; and on the other hand, when new satellites rise above
 320 the cutoff angle, their ambiguities cannot be fixed immediately, which will cause the failure of full
 321 ambiguity resolution.

322 As can be seen in Fig. 6, the number of the fixed ambiguities with a lower success rate is always
 323 larger than those with a higher success rate at the beginning of data processing when full ambiguity
 324 resolution has not been achieved. Besides, full ambiguity resolution with a lower success rate can be
 325 achieved faster than higher success rates. However, the risk of the low success rate is that ambiguities
 326 may not be fixed correctly due to the imprecise model, and wrongly resolved ambiguities may result in

327 unacceptably large position errors (Verhagen et al. 2013). Therefore, it is a trade-off decision for
328 choosing the success rate so that the application scenarios and circumstance need to be carefully
329 considered.

330



331

332

Fig. 6 Number of fixed ambiguities with different success rate criteria for partial ambiguity resolution as compared to all ambiguities. The blue line indicates the number of float ambiguities at each epoch, and the rest of the lines indicate the number of fixed ambiguities in different success rate criteria

334

335

336

337

338

339

340

341

342

343

344

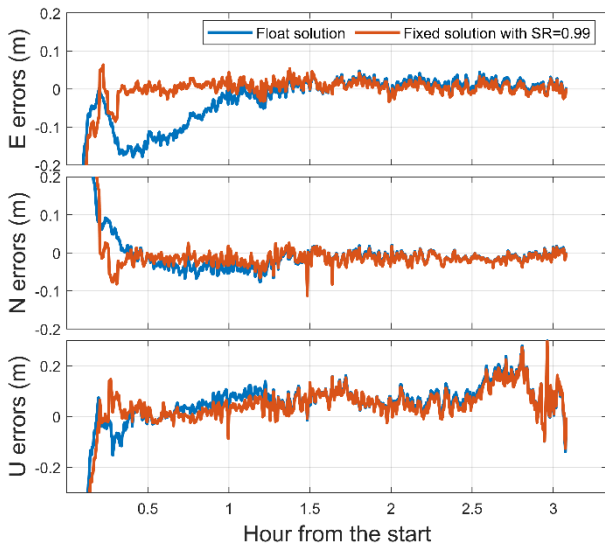
345

Here we present the ambiguity float and fixed positioning solutions under the success rate criterions of 0.99 and 0.99999 in Fig. 7 and Fig. 8, respectively. One can see that in both figures, the ambiguity fixed solutions have a short convergence time as compared to that of the ambiguity float solutions. This is because the horizontal component is highly correlated with ambiguities; therefore, the east and north component can be improved significantly after most of the ambiguities are correctly fixed. Because of the inclined angle of the constellation, it is reasonable to see a significant improvement in the east component because the satellite-receiver geometry on the east-west direction is not as good as that of the north-south due to the trajectory of the satellites; thus the ambiguity float solution of the east component is worse than the north component. However, fixing ambiguity can compensate for the unfavorable geometry in the east-west direction and thus leads to an equal level of accuracy in the east and north component.

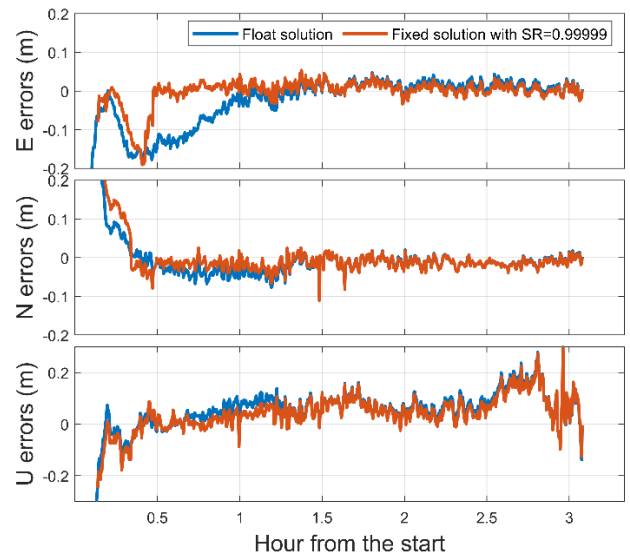
346 For certain epochs at the beginning of data processing for both positioning solutions, the ambiguity
347 fixed solution is close to the float solution because the contribution of ambiguity fixing is not obvious
348 when not too many ambiguities get fixed. Once most integer ambiguities are resolved, i.e., at 0.3 h with
349 the success rate criterion of 0.99 and at 0.5 h with the success rate criterion of 0.99999, which can be
350 seen in Fig. 6, the ambiguity fixed solutions experience a large improvement with the errors being at the
351 centimeter-level, compared to a long convergence time of the ambiguity float positioning errors.

352 One can also see that the first ambiguity fixed solution with the success rate criterion of 0.99999
353 appears later than that with the success rate criterion with the 0.99 because it needs more time for the
354 positioning model to become such strong. However, the positioning solutions with the 0.99 criterion
355 seem to suffer from the wrong fixing ambiguities at around 0.25 h of Fig. 7 because all positioning
356 components have the unexpectedly increased errors at the same period.

357



358
359 Fig. 7 Ambiguity float and fixed positioning
360 errors with the success rate criterion of **0.99**



361
362 Fig. 8 Ambiguity float and fixed positioning
363 errors with the success rate criterion of
364 **0.99999**

365 As can be seen in Fig. 7 and Fig. 8, the ambiguity fixed and float solutions are likewise similar after
 366 a long convergence time, e.g., 1.5 hour. Because the advantage of the fixed ambiguities would not be
 367 obvious when the model has been strong enough. Therefore, the reduced RMSs of the fixed solutions
 368 presented in Table 3 are mainly due to the period 0.5 to 1.5 h since the RMSs are calculated from 0.5 h
 369 to the end, during which the positioning solutions should have been converged. Besides, the fixed
 370 solutions with the two success rate criteria are also almost the same after most ambiguities are fixed.

371 A significant improvement of the ambiguity fixed east component has been demonstrated, and the
 372 north component can also be improved to some extent, even though the ambiguity float north component
 373 has been accurate already. However, it seems that a bias is lumped into the up component and the
 374 integer ambiguity resolution does not benefit the up component much as the horizontal component. This
 375 is because the model strength of the up component in GNSS is weaker than that of the horizontal
 376 component due to the design of the constellation, i.e., all visible satellites are ‘above’ the receiver. This
 377 situation is getting worse for PPP-AR because only one receiver is involved in the data processing.
 378 Meanwhile, it is acknowledged that the geometry of the relative positioning is better than single point
 379 positioning, which means that the reference positions that are obtained by relative positioning must be
 380 better or at least equal to PPP-AR. Therefore, the bias is due to the weak geometry of a single receiver.
 381 Besides, mismodelling tropospheric delay could also affect the solution of the up component because of
 382 the high correlation. Since the double-differenced measurements could to some extent remove
 383 tropospheric model errors, the undifferenced measurements must be influenced by these errors, leading
 384 to a worse up solution as compared to the double-differenced model.

385
 386 Table 3 RMSs of the ambiguity float and fixed solutions with the success rate criteria **0.99** and
 387 **0.99999**

Component	Ambiguity float solution (cm)	Ambiguity fixed solution with the success rate criterion 0.99	Ambiguity fixed solution with the success rate criterion 0.99999
-----------	-------------------------------	---	--

		(cm)	(cm)
E	4.50	1.54	1.55
N	2.65	2.00	1.99
2D	5.22	2.52	2.52
U	8.88	7.89	7.84

388

389

390

391

392

393

394

395

396

397

398

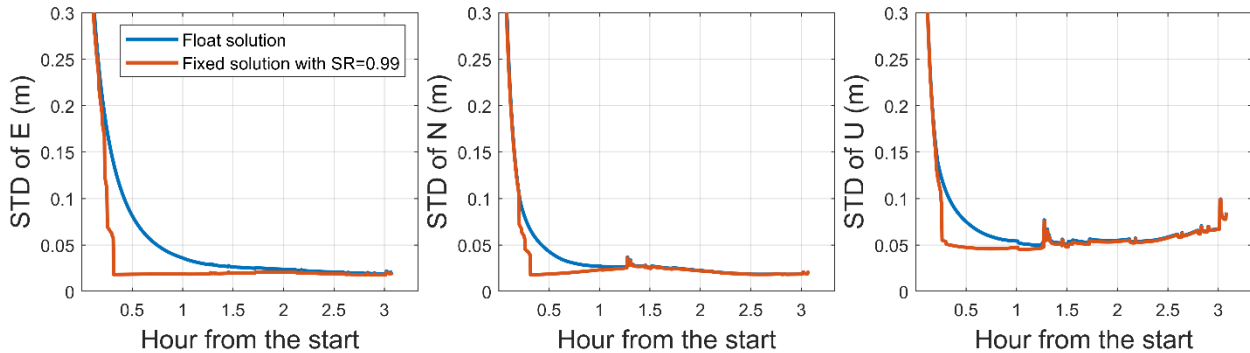
399

400

401

Eq. 8 demonstrates that the precision of the baseline parameters could be improved once the ambiguities are getting fixed. Fig. 9 shows the standard deviations of the positioning components under the ambiguity float solution and fixed solution with the success rate criterion of 0.99. It can be seen that the largest improvement is presented in the east component, which also explains why the east component benefits the most from fixing ambiguities.

Both ambiguity float and fixed STD of the up component are worse than those of the horizontal component because of the design of GNSS, i.e., all satellites are above the receiver. Note that STDs of the up component start rising at 2.5 h and reach a peak value at around 3 h, indicating a bad geometry of the up component during this period. This could be one reason for the bad behavior of the up component within the same period in Fig. 7 and Fig. 8. Another possible reason is the sudden rising attitude of the airplane from 2.5 h and the sudden dropping at 2.8 h (seen in Fig. 2), which causes the residuals of the unmodelled tropospheric delay affecting the up component.



402

403

404

Fig. 9 Standard deviations of the positioning components

405 Process the flight data with **1 s** interval

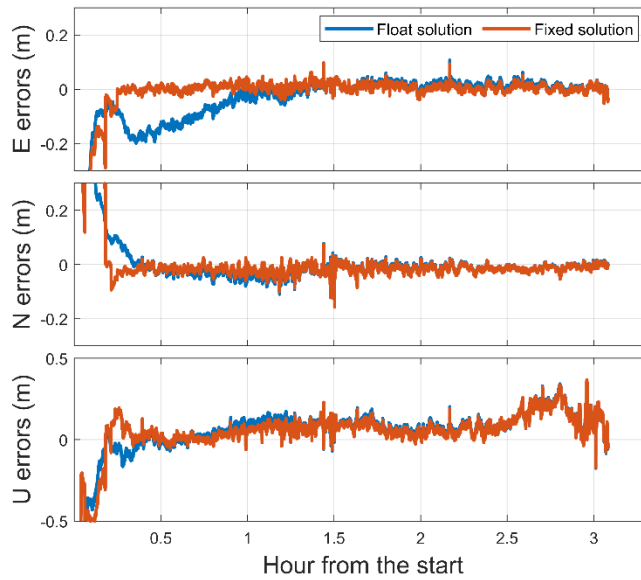
406 One of the issues for processing the flight data with 1 s interval is that the required corrections need
407 to be interpolated from the 15 s to 1 s. We simply implemented the linear interpolation method because
408 of its convenience and efficiency. Among these corrections, the interpolation of the satellite phase bias
409 corrections may not be a problem because they can remain constant over a short time span. However,
410 interpolated satellite clock would be meaningless because the variations of the clock offset are not easily
411 captured and thus not accurately interpolated even during the 15 s period. Therefore, the standard
412 deviations of the phase and code observable are enlarged from 0.005 and 0.5m to 0.01 and 1m,
413 respectively, since the biases of the inaccurate corrections would be lumped into the observables.
414 Besides, the success rate applied in the 1 s interval data test is 0.99999 due to the potentially correlated
415 observations for which the filter cannot handle with. Because the success rate criterion represents how
416 much the precision of the ambiguities can achieve, and thus a higher criterion ensures the successful
417 integer ambiguity resolution to some extent.

418 Fig. **10** shows the ambiguity float and fixed positioning solutions of 1 s interval data processing, in
419 which one can see that the first ambiguity fixed solution appeared earlier than the fixed solutions in Fig.
420 **8** which also applies the 0.99999 success rate. This is because the observations can be quickly
421 accumulated by using a high sample rate, and thus the model strength is able to achieve the high success
422 rate even having the standard deviations of the observables increased. However, fast integer ambiguity
423 resolution does not mean that the ambiguities are fixed correctly. As can be seen in Fig. **10** that the fixed
424 solution of E and N component before 0.25 h show large deviations as compared to the reference
425 positions due to the correlation between ambiguities and horizontal component. This is also the reason
426 for the less impacts on the ambiguity fixed up solution.

427 The accuracy of the up component for ambiguity float and ambiguity fixed solutions are decreased
428 compared to 15 s data processing. This is because the linear interpolation cannot well represent the
429 variations of the clock offsets. Therefore, the satellite clock interpolation and/or prediction need to be
430 further investigated. One can refer to Wang et al. (2017) in which they proposed a dynamic satellite
431 clock incorporated in Kalman filter to predict the clock corrections in a short latency. This model can
432 also be used in interpolating the clock corrections.

433 Unfortunately, even we have known that wrong fixing ambiguities existed in the positioning
434 solutions, we cannot identify which integer ambiguity is not correct. We even do not know which subset
435 of the ambiguity vector is fixed in the partial ambiguity resolution since the original ambiguities have
436 been transformed by Eq. 6 before fixing. Which also indicates that the ‘fixed’ ambiguities may not be
437 integer values if full ambiguity resolution is not performed because the fixed ambiguities need to be
438 computed from the back transformation.

439 It is also worth noting that the successful integer ambiguity resolution starts from 0.25 h in the 1 s
440 interval data processing, which is almost the same as Fig. 7, the 15 s interval. It indicates that other than
441 the model strength, the geometry change is also a key factor for fixing ambiguity. Besides, both the
442 ambiguity float and fixed up solutions of 1 s interval are worse than those of 15 s interval, which can
443 also be seen in Table 4, the RMSs of the positioning solutions of the 1 s interval data processing. The
444 statistics are again calculated from 0.5 h to the end. The worsening of the up component is due to the
445 inaccurate satellite clock corrections.



446
447

Fig. 10 Ambiguity float and fixed positioning solution of **1 s** interval data processing

448
449

Table 4 RMSs of the ambiguity float and fixed solutions in the data processing of **1 s** interval

Component	Ambiguity float solution (cm)	Ambiguity fixed solution (cm)
E	4.47	1.56
N	2.58	2.15
2D	5.16	2.65
U	11.14	10.24

450

451 SUMMARY

452 In this contribution, we implemented the PPP-AR concept in the aviation application since the
 453 technique of integer ambiguity resolution enabled PPP has been widely used in geodetic missions. The
 454 aviation applications may face the challenging circumstances including high velocity and severe
 455 maneuver, and therefore it is worthwhile to investigate if the integer ambiguity resolution is influenced
 456 by such circumstances. An undifferenced and uncombined positioning model which preserves the
 457 integer nature of the ambiguity was applied in network and user side. The satellite clock corrections as
 458 well as the satellite phase bias corrections were generated from the chosen GNSS network and provided
 459 to the flight data, and thus integer ambiguity resolution can be achieved on the receiver of airplane.

460 The flight data was collected from a 3 hours airplane experiment during which intense maneuvers
461 were taken place, and the velocity reached more than 500 km/h. The performance of the PPP-AR was
462 verified in these challenging circumstances with the data processing interval of 15 s and 1 s. And the
463 reference positions are obtained from a relative positioning solution of the TOPCON-TOOLS
464 commercial software with fixed double-differenced ambiguities.

465 The results show that the integer ambiguities can be correctly fixed when the model is strong
466 enough, and the positioning accuracy is improved once most of the ambiguities get fixed, especially for
467 the east component which is highly correlated with the ambiguities. Since the main purpose of fixing
468 ambiguity is to improve the parameters' precision and thus reduce the convergence time, the
469 improvement positioning behavior is mostly due to the period during when the ambiguity fixed solution
470 has been converged, but the ambiguity float solution has not. For the 15 s data test, the accuracy of the
471 horizontal component is improved from 5.22 cm with the ambiguity float to 2.52 cm with the ambiguity
472 fixed solution. However, the improvement for the up component is not obvious, from 8.88 cm to
473 7.98 cm, because the up component is highly correlated with the tropospheric delays and receiver clock
474 offsets.

475 Generally speaking, this PPP-AR procedure performs well in processing the flight data. Both
476 ambiguity float and fixed solution are not significantly affected by the maneuvers of sudden pushovers,
477 accelerations or s-turns. This is because, on the one hand, the positioning model takes into account
478 almost all error sources of GNSS, including the slant ionospheric delay and satellite and receiver phase
479 biases. The realistic model ensures the accuracy of the float ambiguities, and thus they can be fixed
480 successfully. And on the other hand, the Kalman filter can handle the maneuvers very well because the
481 transition matrix of the state updated equation of Kalman filter between consecutive epochs is obtained

482 from the differential equations of the first-order linearized positioning model, and therefore the state
483 transition matrix can well predict the position change between epochs.

484 Several other key issues are also discussed in this contribution. The first one is the influence of the
485 tropospheric delay on the flight data. It is well known that the zenith wet delay should be considered as
486 an unknown parameter and is sensitive to the altitude; therefore, a proper constraint is needed for the
487 process noise of the wet delay as the height of the airplane may dramatically change within a narrow
488 time span. Although the results indicate that a tight constraint of the tropospheric delay is still
489 recommended for the airplane navigation, it could be due to the fact that the reference positions are
490 obtained by a tight troposphere constraint, and thus a small troposphere process noise fits the reference
491 well. However, we can still conclude that the horizontal performance of PPP-AR is comparable with the
492 medium-baseline RTK as the maximum distance between the TOPCON-TOOLS reference receiver and
493 the airplane is 50 km.

494 Secondly, different values of the integer ambiguity resolution success rate criteria are tested and
495 discussed. The success rate is an aspect of the underlying model strength and relates to the number of
496 fixed ambiguities. Since the main systematic errors are taken into account in the positioning model and
497 the flight do not suffered by unexpected situations such as scintillation and weather events, a relatively
498 low success rate criterion (0.99) already works well for the data processing. However, the value of the
499 success rate criterion needs to be determined by the real conditions in different applications.

500 Finally, the flight data is processed in the interval of 1 s, which means that the 1 s corrections are
501 interpolated by the 15 s corrections. The interpolation causes an accuracy degradation of the corrections,
502 especially for the satellite clock because the clock offsets vary quickly even within a very short time
503 span. As a consequence, the up component of the 1 s interval is worse than that of the 15 s interval. And

504 the convergence times for the fixed solutions of the 1 s interval data processing are not shortened
505 because the geometry change is also a key factor for ambiguity fixing.

506 DATA AVAILABILITY STATEMENT

507 Some data used during the study are available online in accordance with funder data retention policies.
508 (Brazilian CORS network):
509 http://geofp.ibge.gov.br/informacoes_sobre_posicionamento_geodesico/rbmc/dados/

510 Some data used during the study were provided by a third party. (Flight test data). Direct request for
511 these materials may be made to the provider (Embraer S.A.) as indicated in the Acknowledgments.

512 ACKNOWLEDGMENTS

513 The first and third authors have received funding from the European Union's Horizon 2020 research and
514 innovation programme under the Marie-Sklodowska Grant Agreement No 722023. The flight test was
515 supported by Embraer S.A. with administration of Agencia Unesp de Inovação (AUIN) and cooperation
516 of Federal University of Pernambuco (UFPE) and São Paulo State University (UNESP).

517 REFERENCES

- 518 Alkan, R. M. (2019). "Cm-level high accurate point positioning with satellite-based GNSS correction
519 service in dynamic applications". *Journal of Spatial Science*, 1-9.
520 <https://doi.org/10.1080/14498596.2019.1643795>
- 521 Chen, X., Allison, T., Cao, W., Ferguson, K., Grünig, S., Gomez, V., Lu, G. (2011, September).
522 "Trimble RTX, an innovative new approach for network RTK". In *proc. 24th International Technical*
523 *Meeting of the Satellite Division of The Institute of Navigation, ION GNSS 2011*. (pp. 2214-2219).
524 Institute of Navigation.
- 525 Dorn, M., Lesjak, R., Huber, K., Wieser, M. (2015). "Improvement of the GNSS Solution for Advanced
526 RPAS Applications Utilizing PPP RTK or Sensor Integration." In *proc. International Micro Air Vehicle*
527 *Conference and Flight Competition (IMAV): Aachen*. (Vol. 15, No. 18).
- 528 Fortes, L. P., Costa, S. M., Abreu, M. A., Silva, A. L., Júnior, N. J., Monico, J. G., Tétréault, P. (2009).
529 "Latest Enhancements in the Brazilian Active Control Network." In *proc. Observing our Changing*
530 *Earth* (pp. 65-70). Springer, Berlin, Heidelberg. https://doi.org/10.1007/978-3-540-85426-5_8
- 531 Ge, M., Gendt, G., Rothacher, M. A., Shi, C., Liu, J. (2008). Resolution of GPS carrier-phase
532 ambiguities in precise point positioning (PPP) with daily observations. *Journal of geodesy*, 82(7), 389-
533 399. <https://doi.org/10.1007/s00190-007-0187-4>
- 534 Geng, J., Teferle, F. N., Meng, X., Dodson, A. H. (2011). Towards PPP-AR: Ambiguity resolution in
535 real-time precise point positioning. *Advances in space research*, 47(10), 1664-1673.
536 <http://doi:10.1016/j.asr.2010.03.030>
- 537 Gottsmann, J., del Potro, R., Muller, C. (2018). "50 years of steady ground deformation in the Altiplano-
538 Puna region of southern Bolivia." *Geosphere*, 14(1), 65-73. <https://doi.org/10.1130/GES01570.1>

539 Hou, Y., Verhagen, S., Wu, J. (2016). "A data driven partial ambiguity resolution: Two step success rate
540 criterion, and its simulation demonstration." *Advances in Space Research*, 58(11), 2435-2452.
541 <https://doi.org/10.1016/j.asr.2016.07.029>

542 Imparato, D. (2016). "GNSS Based Receiver Autonomous Integrity Monitoring for Aircraft Navigation."
543 TU Delft: Delft, The Netherlands. <https://doi.org/10.4233/uuid:a5e5f5be-b1a6-42c2-b285-a4ff01e5bfd2>

544 Kouba, J., Héroux, P. (2001). "Precise point positioning using IGS orbit and clock products." *GPS*
545 *solutions*, 5(2), 12-28. <https://doi.org/10.1007/PL00012883>

546 Li, B., Verhagen, S., Teunissen, P. J. (2014). "Robustness of GNSS integer ambiguity resolution in the
547 presence of atmospheric biases." *GPS solutions*, 18(2), 283-296. [https://doi.org/10.1007/s10291-013-](https://doi.org/10.1007/s10291-013-0329-5)
548 [0329-5](https://doi.org/10.1007/s10291-013-0329-5)

549 Li, X., Ge, M., Zhang, H., Wickert, J. (2013). A method for improving uncalibrated phase delay
550 estimation and ambiguity-fixing in real-time precise point positioning. *Journal of Geodesy*, 87(5), 405-
551 416. <https://doi.org/10.1007/s00190-013-0611-x>

552 Liu, X., Goode, M., Tegedor, J., Vigen, E., Oerpen, O., Strandli, R. (2015, October). "Real-time multi-
553 constellation precise point positioning with integer ambiguity resolution." In *proc. 2015 International*
554 *association of institutes of navigation world congress (IAIN)* (pp. 1-7). IEEE.

555 Ma, H., Antoniou, M., Cherniakov, M., Pastina, D., Santi, F., Pieralice, F., Bucciarelli, M. (2017).
556 "Maritime target detection using GNSS-based radar: Experimental proof of concept." In *proc. 2017*
557 *IEEE Radar Conference (RadarConf)* (pp. 0464-0469). IEEE.
558 <https://doi.org/10.1109/RADAR.2017.7944248>

559 Ma, H., Zhao, Q., Verhagen, S., Psychas, D., Liu, X. (2020). "Assessing the Performance of Multi-
560 GNSS PPP-AR in the Local Area." *Remote Sensing*. 12, 3343. <https://doi.org/10.3390/rs12203343>

561 Monico, J. F. G., Marques, H. A., Tsuchiya, Í., Oyama, R. T., Queiroz, W. R. S. D., Souza, M. C. D.,
562 Wentz, J. P. (2019). "Real time PPP applied to airplane flight tests." *Boletim de Ciências Geodésicas*,
563 25(2). <https://doi.org/10.1590/s1982-21702019000200009>

564 Nadarajah, N., Khodabandeh, A., Wang, K., Choudhury, M., Teunissen, P. J. (2018). "Multi-GNSS PPP-
565 AR: from large-to small-scale networks." *Sensors*, 18(4), 1078-1093. <https://doi.org/10.3390/s18041078>

566 Odijk, D. (2003). "Ionosphere-free phase combinations for modernized GPS." *Journal of surveying*
567 *engineering*, 129(4), 165-173. [https://doi.org/10.1061/\(ASCE\)0733-9453\(2003\)129:4\(165\)](https://doi.org/10.1061/(ASCE)0733-9453(2003)129:4(165))

568 Odijk, D., Khodabandeh, A., Nadarajah, N., Choudhury, M., Zhang, B., Li, W., Teunissen, P. J. (2017).
569 "PPP-AR by means of S-system theory: Australian network and user demonstration." *Journal of Spatial*
570 *Science*, 62(1), 3-27. <https://doi.org/10.1080/14498596.2016.1261373>

571 Odijk, D., Teunissen, P. J., Khodabandeh, A. (2014). "Single-frequency PPP-AR: theory and
572 experimental results." *Proceedings in Earth on the edge: Science for a sustainable planet* (pp. 571-578).
573 Springer, Berlin, Heidelberg. https://doi.org/10.1007/978-3-642-37222-3_75

574 Odijk, D., Zhang, B., Khodabandeh, A., Odolinski, R., Teunissen, P. J. (2016). "On the estimability of
575 parameters in undifferenced, uncombined GN network and PPP-AR user models by means of S-system
576 theory." *Journal of Geodesy*, 90(1), 15-44. <https://doi.org/10.1007/s00190-015-0854-9>

577 Prabha, C., Sunitha, R., Anitha, R. (2014). "Automatic vehicle accident detection and messaging system
578 using gsm and GPS modem." In *proc. International Journal of Advanced Research in Electrical,*
579 *Electronics and Instrumentation Engineering*, 3(7), 10723-10727.
580 <https://doi.org/10.15662/ijareeie.2014.0307062>

581 Psychas, D., Bruno, J., Massarweh, L., Darugna, F. (2019). "Towards Sub-meter Positioning using
582 Android Raw GNSS Measurements." In *proc 32nd International Technical Meeting of the Satellite*
583 *Division of the Institute of Navigation, ION GNSS+ 2019* (pp. 3917-3931). Institute of Navigation.
584 <https://doi.org/10.33012/2019.17077>

585 Richter, A., Ivins, E., Lange, H., Mendoza, L., Schröder, L., Hormaechea, J. L., Horwath, M. (2016).
586 "Crustal deformation across the Southern Patagonian Icefield observed by GNSS." *Earth and Planetary*
587 *Science Letters*, 452, 206-215. <https://doi.org/10.1016/j.epsl.2016.07.042>

588 Roberts, P., Walker, R., O'Shea, P. (2005). "Fixed wing UAV navigation and control through integrated
589 GNSS and vision." In *proc. AIAA guidance, navigation, and control conference and exhibit* (pp. 5867).
590 <https://doi.org/10.2514/6.2005-5867>

591 Saastamoinen, J. (1972). "Atmospheric correction for the troposphere and stratosphere in radio ranging
592 satellites." *The use of artificial satellites for geodesy*, 15, 247-251. <https://doi.org/10.1029/GM015p0247>

593 Severi, S., Härrri, J., Ulmschneider, M., Denis, B., Bartels, M. (2018). "Beyond GNSS: Highly accurate
594 localization for cooperative-intelligent transport systems." In *proc. 2018 IEEE Wireless Communications*
595 *and Networking Conference (WCNC)* (pp. 1-6). IEEE. <https://doi.org/10.1109/WCNC.2018.8377457>

596 Tegedor, J., Liu, X., De Jong, K., Goode, M., Øvstedal, O., Vigen, E. (2016). "Estimation of Galileo
597 Uncalibrated Hardware Delays for Ambiguity-Fixed Precise Point Positioning." *Navigation: Journal of*
598 *The Institute of Navigation*, 63(2), 173-179.

599 Teunissen, P. J. (2000). "The success rate and precision of GPS ambiguities." *Journal of Geodesy*, 74(3-
600 4), 321-326. <https://doi.org/10.1007/s001900050289>

601 Teunissen, P. J. (1993). "Least-squares estimation of the integer GPS ambiguities." In *proc. Invited*
602 *lecture, section IV theory and methodology*, IAG general meeting, Beijing, China.

603 Teunissen, P. J. (1995). "The least-squares ambiguity decorrelation adjustment: a method for fast GPS
604 integer ambiguity estimation." *Journal of Geodesy*, 70(1), 65-82. <https://doi.org/10.1007/BF00863419>

605 Teunissen, P. J. (1998a). "GPS carrier phase ambiguity fixing concepts." In *GPS for Geodesy* (pp. 319-
606 388). Springer, Berlin, Heidelberg. https://doi.org/10.1007/978-3-642-72011-6_8

607 Teunissen, P. J. (1998b). "Success probability of integer GPS ambiguity rounding and bootstrapping."
608 *Journal of Geodesy*, 72(10), 606-612. <https://doi.org/10.1007/s001900050199>

609 Teunissen, P. J. G. (1998c). "The distribution of the GPS baseline in case of integer least-squares
610 ambiguity estimation." *Artificial Satellites*, 33(2), 65-75.

611 Teunissen, P. J., De Jonge, P. J., Tiberius, C. C. J. M. (1997). "Performance of the LAMBDA method
612 for fast GPS ambiguity resolution." *Navigation*, 44(3), 373-383.

613 Teunissen, P. J., Giorgi, G., Buist, P. J. (2011). "Testing of a new single-frequency GNSS carrier phase
614 attitude determination method: land, ship and aircraft experiments." *GPS solutions*, 15(1), 15-28.
615 <https://doi.org/10.1007/s10291-010-0164-x>

616 Teunissen, P. J., Khodabandeh, A. (2015). "Review and principles of PPP-AR methods." *Journal of*
617 *Geodesy*, 89(3), 217-240. <https://doi.org/10.1007/s00190-014-0771-3>

618 Teunissen, P. J., Kleusberg, A. (Eds.). (2012). *GPS for Geodesy*. (pp. 182-184). Springer Science &
619 Business Media.

620 Teunissen, P. J., Odijk, D., Zhang, B. (2010). "PPP-AR: results of CORS network-based PPP with
621 integer ambiguity resolution." *J Aeronaut Astronaut Aviat Ser A*, 42(4), 223-230.

622 Teunissen, P., De Jonge, P., Tiberius, C. C. J. M. (1996). "The Volume of the GPS Ambiguity Search
623 Space and its Relevance for Integer Ambiguity Resolution." In *proc. the 9th International Technical*
624 *Meeting of the Satellite Division, ION GPS* (Vol. 9, pp. 889-898). Institute of navigation.

625 Teunissen, P.J.G., (2000). "On the GNSS Integer Ambiguity Success Rate." *Lustumboek Snellius*, The
626 5th Element: 103–108

627 Verhagen, S., Li, B., Teunissen, P. J. (2013). "Ps-LAMBDA: ambiguity success rate evaluation software
628 for interferometric applications." *Computers & Geosciences*, 54, 361-376.
629 <https://doi.org/10.1016/j.cageo.2013.01.014>

630 Verhagen, S., Teunissen, P. (2004). On the foundation of the popular ratio test for GNSS ambiguity
631 resolution. In *proc. the 17th International Technical Meeting of the Satellite Division, ION GPS* (Vol. 17,
632 pp. 2529-2540). Institute of navigation.

633 Verhagen, S., Teunissen, P. J. (2017). "Least-squares estimation and Kalman filtering." In *Springer*
634 *Handbook of Global Navigation Satellite Systems* (pp. 639-660). Springer, Cham.
635 https://doi.org/10.1007/978-3-319-42928-1_22

636 Verhagen, S., Teunissen, P. J., van der Marel, H., & Li, B. (2011). "GNSS ambiguity resolution: which
637 subset to fix." In *proc. International Global Navigation Satellite Systems Society, IGNSS Symposium*, 1–
638 15.

639 Wang, K., Khodabandeh, A., Teunissen, P. (2017). "A study on predicting network corrections in PPP-
640 AR processing." *Advances in Space Research*, 60(7), 1463-1477.
641 <https://doi.org/10.1016/j.asr.2017.06.043>

642 Wang, L., Verhagen, S. (2015). A new ambiguity acceptance test threshold determination method with
643 controllable failure rate. *Journal of Geodesy*, 89(4), 361-375. doi:10.1007/s00190-014-0780-2

644 Wu, Q., Sun, M., Zhou, C., Zhang, P. (2019). "Precise point positioning using dual-frequency GNSS
645 observations on smartphone." *Sensors*, 19(9), 2189-2206. <https://doi.org/10.3390/s19092189>

646 Zhang, B., Teunissen, P. J., Odijk, D. (2011). "A novel un-differenced PPP-AR concept." *The Journal of*
647 *Navigation*, 64(S1), 180-191. <https://doi.org/10.1017/S0373463311000361>

648 Zumberge, J. F., Heflin, M. B., Jefferson, D. C., Watkins, M. M., Webb, F. H. (1997). "Precise point
649 positioning for the efficient and robust analysis of GPS data from large networks." *Journal of*
650 *geophysical research: solid earth*, 102(B3), 5005-5017. <https://doi.org/10.1029/96JB03860>